Computers and Mathematics with Applications 59 (2010) 457–467

Contents lists available at ScienceDirect

Computers and Mathematics with Applications

journal homepage: www.elsevier.com/locate/camwa

C^1 positive scattered data interpolation

Malik Zawwar Hussain *, Maria Hussain

Department of Mathematics, University of the Punjab, 54590 Lahore, Pakistan

ARTICLE INFO

Article history:
Received 11 March 2009
Accepted 22 June 2009

Keywords:
Triangular surface patch
Rational cubic function
Free parameters
Positive scattered data

ABSTRACT

A local C^1 surface construction scheme is presented to preserve the shape of positive scattered data arranged over a triangular grid. Each boundary curve of the triangle is constructed by a rational cubic function with two free parameters, and this rational function is also used for the side-vertex interpolation. The final surface patch is constructed by taking the convex combination of three side-vertex interpolants. For each triangular patch there are three boundary curves and three side-vertex interpolants. Simple sufficient data dependent constraints are derived on these free parameters to preserve the shape of the positive scattered data. The developed scheme is not only local and computationally economical but visually pleasing as well.

1. Introduction

Positivity is an important shape property. There are many physical situations where entities only have a meaning when their values are positive. In mineral exploration, exploratory wells are drilled and depths of various layers are recorded. Obviously, the depth of the surface cannot be negative. Pressure with derivatives is used to visualize the far-field pattern of four-point sources. Other application areas include monthly rainfall amounts, levels of gas discharge in certain chemical reactions, progress of an irreversible process, resistance offered by an electric circuit, volume, density, etc. This paper is particularly concerned with the construction of interpolating surfaces that preserve the positivity of scattered data.

The problem of shape preservation of positive scattered data has been discussed by a number of authors. Asim, Mustafa and Brodlie [1] visualized positive scattered data subject to global positivity constraints using a modified quadratic Shepard method. Positivity was achieved by scaling the basis functions as far as was necessary. Chan and Ong [2] described a local scheme for range restricted C^1 interpolation of scattered data. The interpolating surface is a piecewise convex rational combination of three cubic Bézier patches. Sufficient conditions for the non-negativity of a cubic Bézier triangle were derived and used as lower bounds on the Bézier ordinates. If the Bézier ordinates did not satisfy the derived lower bounds, then non-negativity could be achieved by modifying the first-order partial derivatives at data sites. Kong, Ong and Saw [3] discussed the problem of range restricted scattered data interpolation using triangles. Each triangle of the Delaunay triangulated domain is split into three and each sub-triangle is interpolated using a cubic Bézier triangular patch. The non-negativity is expressed as lower bounds to Bézier ordinates. In [3], if the Bézier ordinates fail to satisfy derived lower bounds for non-negativity then these are rescaled by modifying the first-order partial derivatives at data sites to achieve non-negativity. Mulansky and Schmidt [4] proposed a C^1 non-negativity preserving scheme by using a quadratic spline interpolant on the Powell–Sabin refinement of the Delaunay triangulation of the data sites. The non-negativity constraints give rise to a system of linear inequalities with gradients as parameters. The selection of a suitable solution is based on the minimization of a thin

* Corresponding author. Tel.: +92 300 9422346.
E-mail address: malikzawwar@math.pu.edu.pk (M.Z. Hussain).

0898-1221/$ – see front matter © 2009 Elsevier Ltd. All rights reserved.
doi:10.1016/j.camwa.2009.06.019

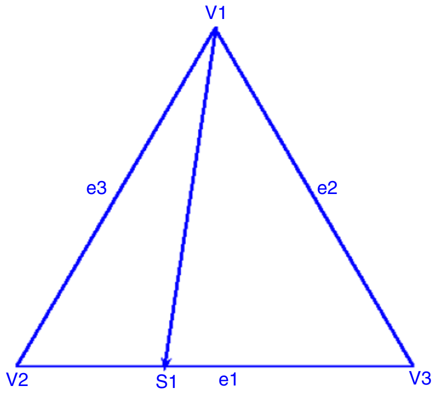

Fig. 1. Locations of the vertices and edges of the triangle $\triangle V_1V_2V_3$.

plate energy functional. In [2–4], constraints are derived on derivatives. So, whilst all these schemes are local, they will not work if the data are given with the derivatives.

Ong and Wong [5] used the side-vertex method for interpolation on a triangle. Each triangular patch is a convex combination of three side-vertex interpolants. A 1-parameter rational cubic function is used as a side-vertex interpolant. The value of the free parameter that reduces the rational cubic function to a cubic Hermite is used in all the triangular patches. If the Hermite triangular patches lose positivity, a global maximum value is assigned to all parameters of each triangle interpolant to ensure that the resulting surface is non-negative. Hence, although this method works with both data and derivatives, it is non-local.

Piah, Goodman and Unsworth [6] constructed the interpolating surfaces comprising cubic Bézier triangular patches. They imposed sufficient conditions on the ordinates of the Bézier control net in each triangle to ensure positivity. The derivatives at the data points are determined to be consistent with these conditions. The disadvantage of the scheme is that actual derivatives cannot be supplied.

The problems of positive and monotone curve data interpolation were discussed in [13] and [16] respectively. In [14,15], the problem of scattered data interpolation was addressed.

This paper is concerned with positivity preserving triangle-based interpolation of scattered data using a C^1 and local side-vertex method that is applicable to data both with and without derivatives. The C^1 piecewise rational cubic function is used for both the boundary and the side-vertex interpolant. The rational function possesses two free parameters, yielding 12 free parameters over each triangular patch. Positivity is achieved by deriving simple sufficient data dependent constraints on these free parameters. The developed scheme is demonstrated graphically.

The remainder of the paper is organized as follows. Section 2 describes the C^1 side-vertex method for interpolation over a triangle. Section 3 details the piecewise rational cubic function to be used. The positivity problem is discussed in Section 4 for the generation of a C^1 positivity preserving scattered data interpolant. The surface scheme is demonstrated in Section 5. Finally, Section 6 discusses some of the results from Section 4 and concludes the paper.

2. C^1 side-vertex method for interpolation over a triangle

Let $\{(x_i, y_i, F_i), i = 1, 2, 3, \dots, n\}$ be the given scattered data arranged over the triangular grid.

For a non-degenerate triangle $T = \triangle V_1V_2V_3$, with vertices $\{V_i = (x_i, y_i), i = 1, 2, 3\}$ and barycentric coordinates u, v and w, any point $V = (x, y)$ on the triangle can be expressed as (Fig. 1)

$$V = uV_1 + vV_2 + wV_3, \tag{1}$$

where

$$u + v + w = 1 \quad \text{and} \quad u, v, w \geq 0. \tag{2}$$

In this paper we used a C^1 interpolant [7] over each triangular patch, defined by the following convex combination:

$$P(u, v, w) = \frac{v^2w^2P_1 + u^2w^2P_2 + u^2v^2P_3}{v^2w^2 + u^2w^2 + u^2v^2}, \tag{3}$$

where the P_i's are the radial curves connecting vertices V_i's with a point on the opposite boundary edge. The interpolant (3) not only interpolates data values at the vertices but the first-order derivative at the boundary edges as well.

At the vertices of the triangle $\triangle V_1V_2V_3$ where two of the barycentric coordinates are simultaneously zero, the interpolant (3) is defined as

$$P(u, v, w) = F_1 \quad \text{when } v = w = 0,$$
$$P(u, v, w) = F_2 \quad \text{when } u = w = 0,$$
$$P(u, v, w) = F_3 \quad \text{when } v = u = 0,$$

where $F_i, i = 1, 2, 3$ are the ordinate values at the vertices $V_i = (x_i, y_i), i = 1, 2, 3$.

3. Rational cubic function

In this paper we use the rational cubic function of [8] and adopt the approach of [9] in describing it.

Let $(x_i, f_i), i = 0, 1, 2, \ldots, n$ be a given set of data points, where $x_0 < x_1 < \cdots < x_n$. A piecewise rational cubic function is defined over each interval $I_i = [x_i, x_{i+1}]$ as

$$S(x) = \frac{p_i(\theta)}{q_i(\theta)}, \tag{4}$$

where

$$p_i(\theta) = (1-\theta)^3 \eta_i f_i + (1-\theta)^2 \theta \{(2\eta_i\chi_i + \eta_i) f_i + \eta_i h_i d_i\} + (1-\theta)\theta^2 \{(2\eta_i\chi_i + \chi_i) f_{i+1} - \chi_i h_i d_{i+1}\} + \theta^3 \chi_i f_{i+1},$$
$$q_i(\theta) = (1-\theta)^2 \eta_i + 2(1-\theta)\theta\eta_i\chi_i + \theta^2\chi_i,$$
$$\theta = \frac{x - x_i}{h_i}, \quad h_i = x_{i+1} - x_i.$$

The rational cubic (4) has the following properties:

$$S(x_i) = f_i, \qquad S(x_{i+1}) = f_{i+1}, \qquad S^{(1)}(x_i) = d_i, \qquad S^{(1)}(x_{i+1}) = d_{i+1}.$$

$S^{(1)}(x)$ denotes the derivative with respect to x and d_i denotes derivative values (given or estimated by some method) at knot x_i. $S(x) \in C^1[x_0, x_n]$ has η_i and χ_i as free parameters in the interval $I_i = [x_i, x_{i+1}]$. It is noted that in each interval I_i, when $\eta_i = 1$ and $\chi_i = 1$, the piecewise rational cubic function reduces to the standard cubic Hermite.

Hussain and Ali in [10] developed the following result:

Theorem 1. *The piecewise rational cubic function (4) preserves positivity if the free parameters η_i and χ_i satisfy the following condition in each interval $[x_i, x_{i+1}]$:*

$$\eta_i > \text{Max}\left\{0, \frac{h_i d_{i+1}}{2f_{i+1}}\right\} \quad \textit{and} \quad \chi_i > \text{Max}\left\{0, -\frac{h_i d_i}{2f_i}\right\}.$$

4. The C^1 positivity preserving scattered data interpolation

The positivity preserving scattered data interpolation problem is described as follows.

Let $\{(x_i, y_i, F_i), i = 1, 2, 3, \ldots, n\}$ be the given positive scattered data points, i.e. $F_i > 0, i = 1, 2, 3, \ldots, n$. The conditions for $S(x, y)$ being positive over the whole domain D are

$$S(x_i, y_i) = F_i, \quad i = 1, 2, \ldots, n$$
$$S(x, y) > 0, \quad \forall\ (x, y) \in D.$$

4.1. Triangulation

The domain is triangulated by the Delaunay triangulation method [11] such that the data F_i are lying at the vertices $V_i = (x_i, y_i)$, $i = 1, 2, 3, \ldots, n$ of the triangles.

4.2. Estimation of derivatives

Partial derivatives at the vertices $V_i, i = 1, 2, 3$ are estimated by the derivative estimation technique proposed in [12].

4.3. The C^1 positive triangular patch

Let $\triangle V_1V_2V_3$ be the given triangle having edges $e_i, i = 1, 2, 3$ opposite to the vertices $V_i, i = 1, 2, 3$, respectively.

The radial curve P_1 connecting a vertex V_1 to the point S_1 on the opposite edge e_1 is defined as

$$P_1 = \frac{P_{1n}}{P_{1d}}, \tag{5}$$

where

$$P_{1n} = \left\{(1-u)^3\beta_i + (1-u)^2 uA_2\right\} F(S_1) + \alpha_i F_1 + vD_1 + wD_2 + v^2D_3 + vwD_4 + w^2D_5 + v^3D_6 + v^2wD_7 + vw^2D_8 + w^3D_9, \tag{6}$$

$$P_{1d} = \alpha_i u^2 + 2\alpha_i\beta_i(1-u)u + \beta_i(1-u)^2, \tag{7}$$

$$\begin{aligned}
D_1 &= -3\alpha_i F_1 + A_1F_1 + \alpha_i R_3,\\
D_2 &= -3\alpha_i F_1 + A_1F_1 + \alpha_i R_4,\\
D_3 &= 3\alpha_i F_1 - 2A_1F_1 - \beta_i R_1 - 2\alpha_i R_3,\\
D_4 &= 6\alpha_i F_1 - 4A_1F_1 - \beta_i R_1 - \beta_i R_2 - 2\alpha_i R_3 - 2\alpha_i R_4,\\
D_5 &= 3\alpha_i F_1 - 2A_1F_1 - \beta_i R_2 - 2\alpha_i R_4,\\
D_6 &= -\alpha_i F_1 + A_1F_1 + \beta_i R_1 + \alpha_i R_3,\\
D_7 &= -3\alpha_i F_1 + 3A_1F_1 + 2\beta_i R_1 + \beta_i R_2 + 2\alpha_i R_3 + \alpha_i R_4,\\
D_8 &= -3\alpha_i F_1 + 3A_1F_1 + \beta_i R_1 + 2\beta_i R_2 + \alpha_i R_3 + 2\alpha_i R_4,\\
D_9 &= -\alpha_i F_1 + A_1F_1 + \beta_i R_2 + \alpha_i R_4,
\end{aligned}$$

$$R_1 = (x_2-x_1)\frac{\partial F}{\partial x}(S_1) + (y_2-y_1)\frac{\partial F}{\partial y}(S_1), \qquad R_2 = (x_3-x_1)\frac{\partial F}{\partial x}(S_1) + (y_3-y_1)\frac{\partial F}{\partial y}(S_1),$$

$$R_3 = (x_2-x_1)\frac{\partial F}{\partial x}(V_1) + (y_2-y_1)\frac{\partial F}{\partial y}(V_1), \qquad R_4 = (x_3-x_1)\frac{\partial F}{\partial x}(V_1) + (y_3-y_1)\frac{\partial F}{\partial y}(V_1),$$

$$A_1 = (2\alpha_i\beta_i + \alpha_i), \qquad A_2 = (2\alpha_i\beta_i + \beta_i),$$

$$F(S_1) = \frac{\gamma_1F_2r^3 + \{(2\gamma_1\delta_1+\gamma_1)F_2 + \gamma_1d_3\}r^2r_1 + \{(2\gamma_1\delta_1+\delta_1)F_3 - \delta_1d_4\}rr_1^2 + \delta_1F_3r_1^3}{\gamma_1r^2 + 2\gamma_1\delta_1rr_1 + \delta_1r_1^2}, \tag{8}$$

$$d_3 = (x_3-x_2)\frac{\partial F}{\partial x}(V_2) + (y_3-y_2)\frac{\partial F}{\partial y}(V_2), \qquad d_4 = (x_3-x_2)\frac{\partial F}{\partial x}(V_3) + (y_3-y_2)\frac{\partial F}{\partial y}(V_3),$$

$$r = \frac{v}{v+w}, \qquad r_1 = \frac{w}{v+w}.$$

Similarly, the radial curves P_2 and P_3 connecting the vertices V_2 and V_3 to the points S_2 and S_3 on the opposite edges e_2 and e_3 are defined as

$$P_2 = \frac{P_{2n}}{P_{2d}}, \tag{9}$$

where

$$P_{2n} = \left\{(1-v)^3\beta_j + (1-v)^2 vB_2\right\} F(S_2) + \alpha_j F_2 + uE_1 + wE_2 + u^2E_3 + uwE_4 + w^2E_5 + u^3E_6 + u^2wE_7 + uw^2E_8 + w^3E_9, \tag{10}$$

$$P_{2d} = \alpha_j v^2 + 2\alpha_j\beta_j(1-v)v + \beta_j(1-v)^2, \tag{11}$$

where

$$\begin{aligned}
E_1 &= -3\alpha_j F_2 + B_1F_2 + \alpha_j R_7,\\
E_2 &= -3\alpha_j F_2 + B_1F_2 + \alpha_j R_8,\\
E_3 &= 3\alpha_j F_2 - 2B_1F_2 - \beta_j R_5 - 2\alpha_j R_7,\\
E_4 &= 6\alpha_j F_2 - 4B_1F_2 - \beta_j R_5 - \beta_j R_6 - 2\alpha_j R_7 - 2\alpha_j R_8,\\
E_5 &= 3\alpha_j F_2 - 2B_1F_2 - \beta_j R_6 - 2\alpha_j R_8,\\
E_6 &= -\alpha_j F_2 + B_1F_2 + \beta_j R_5 + \alpha_j R_7,\\
E_7 &= -3\alpha_j F_2 + 3B_1F_2 + 2\beta_j R_5 + \beta_j R_6 + 2\alpha_j R_7 + \alpha_j R_8,\\
E_8 &= -3\alpha_j F_2 + 3B_1F_2 + \beta_j R_5 + 2\beta_j R_6 + \alpha_j R_7 + 2\alpha_j R_8,\\
E_9 &= -\alpha_j F_2 + B_1F_2 + \beta_j R_6 + \alpha_j R_8,
\end{aligned}$$

$$R_5 = (x_1-x_2)\frac{\partial F}{\partial x}(S_2) + (y_1-y_2)\frac{\partial F}{\partial y}(S_2), \qquad R_6 = (x_3-x_2)\frac{\partial F}{\partial x}(S_2) + (y_3-y_2)\frac{\partial F}{\partial y}(S_2),$$

$$R_7 = (x_1-x_2)\frac{\partial F}{\partial x}(V_2) + (y_1-y_2)\frac{\partial F}{\partial y}(V_2), \qquad R_8 = (x_3-x_2)\frac{\partial F}{\partial x}(V_2) + (y_3-y_2)\frac{\partial F}{\partial y}(V_2),$$

$$B_1 = \left(2\alpha_j\beta_j + \alpha_j\right), \qquad B_2 = \left(2\alpha_j\beta_j + \beta_j\right),$$

$$F\left(S_2\right)=\frac{\gamma_2 F_3 s_1^3+\left\{\left(2\gamma_2\delta_2+\gamma_2\right)F_3+\gamma_2 d_5\right\}s_1^2 s+\left\{\left(2\gamma_2\delta_2+\delta_2\right)F_1-\delta_2 d_6\right\}s_1 s^2+\delta_2 F_1 s^3}{\gamma_2 s_1^2+2\gamma_2\delta_2 s_1 s+\delta_2 s^2}, \tag{12}$$

$$d_5=\left(x_1-x_3\right)\frac{\partial F}{\partial x}\left(V_3\right)+\left(y_1-y_3\right)\frac{\partial F}{\partial y}\left(V_3\right), \qquad d_6=\left(x_1-x_3\right)\frac{\partial F}{\partial x}\left(V_1\right)+\left(y_1-y_3\right)\frac{\partial F}{\partial y}\left(V_1\right),$$

$$s_1=\frac{w}{u+w}, \qquad s=\frac{u}{u+w}.$$

$$P_3=\frac{P_{3n}}{P_{3d}}, \tag{13}$$

where

$$P_{3n} = \left\{(1-w)^3\beta_k+(1-w)^2 wC_2\right\}F(S_3)+\alpha_k F_3+uG_1+vG_2 + u^2G_3+uvG_4+v^2G_5+u^3G_6+u^2vG_7+uv^2G_8+v^3G_9, \tag{14}$$

$$P_{3d}=\alpha_k w^2+2\alpha_k\beta_k\left(1-w\right)w+\beta_k\left(1-w\right)^2, \tag{15}$$

where

$$G_1=-3\alpha_k F_3+C_1F_3+\alpha_k R_{11},$$
$$G_2=-3\alpha_k F_3+C_1F_3+\alpha_k R_{12},$$
$$G_3=3\alpha_k F_3-2C_1F_3-\beta_k R_9-2\alpha_k R_{11},$$
$$G_4=6\alpha_k F_3-4C_1F_3-\beta_k R_9-\beta_k R_{10}-2\alpha_k R_{11}-2\alpha_k R_{12},$$
$$G_5=3\alpha_k F_3-2C_1F_3-\beta_k R_{10}-2\alpha_k R_{12},$$
$$G_6=-\alpha_k F_3+C_1F_3+\beta_k R_9+\alpha_k R_{11},$$
$$G_7=-3\alpha_k F_3+3C_1F_3+2\beta_k R_9+\beta_k R_{10}+2\alpha_k R_{11}+\alpha_k R_{12}$$
$$G_8=-3\alpha_k F_3+3C_1F_3+\beta_k R_9+2\beta_k R_{10}+\alpha_k R_{11}+2\alpha_k R_{12},$$
$$G_9=-\alpha_k F_3+C_1F_3+\beta_k R_{10}+\alpha_k R_{12},$$
$$R_9=\left(x_1-x_3\right)\frac{\partial F}{\partial x}\left(V_3\right)+\left(y_1-y_3\right)\frac{\partial F}{\partial y}\left(V_3\right), \qquad R_{10}=\left(x_2-x_3\right)\frac{\partial F}{\partial x}\left(V_3\right)+\left(y_2-y_3\right)\frac{\partial F}{\partial y}\left(V_3\right),$$
$$R_{11}=\left(x_1-x_3\right)\frac{\partial F}{\partial x}\left(S_3\right)+\left(y_1-y_3\right)\frac{\partial F}{\partial y}\left(S_3\right), \qquad R_{12}=\left(x_2-x_3\right)\frac{\partial F}{\partial x}\left(S_3\right)+\left(y_2-y_3\right)\frac{\partial F}{\partial y}\left(S_3\right),$$
$$C_1=\left(2\alpha_k\beta_k+\alpha_k\right), \qquad C_2=\left(2\alpha_k\beta_k+\beta_k\right),$$

$$F\left(S_3\right)=\frac{\gamma_3 F_1 t_1^3+\left\{\left(2\gamma_3\delta_3+\gamma_3\right)F_1+\gamma_3 d_1\right\}t_1^2 t+\left\{\left(2\gamma_3\delta_3+\delta_3\right)F_2-\delta_3 d_2\right\}t_1 t^2+\delta_3 F_2 t^3}{\gamma_3 t_1^2+2\gamma_3\delta_3 t_1 t+\delta_3 t^2}, \tag{16}$$

$$d_1=\left(x_2-x_1\right)\frac{\partial F}{\partial x}\left(V_1\right)+\left(y_2-y_1\right)\frac{\partial F}{\partial y}\left(V_1\right), \qquad d_2=\left(x_2-x_1\right)\frac{\partial F}{\partial x}\left(V_2\right)+\left(y_2-y_1\right)\frac{\partial F}{\partial y}\left(V_2\right),$$

$$t_1=\frac{u}{u+v}, \quad t=\frac{v}{u+v}.$$

From (5), $P_1>0$ if $P_{1n}>0$ and $P_{1d}>0$.
From (6), $P_{1n}>0$ if $\alpha_i>0$, $\beta_i>0$, $F\left(S_1\right)>0$ and $D_i>0$, $i=1,2,3,\ldots,9$.
From (7), $P_{1d}>0$ if $\alpha_i>0$ and $\beta_i>0$.
From Theorem 1, $F\left(S_1\right)>0$ if $\gamma_1>\text{Max}\left\{0,\frac{d_4}{2F_3}\right\}$ and $\delta_1>\text{Max}\left\{0,-\frac{d_3}{2F_2}\right\}$.

$$D_i>0, \quad i=1,2,3,\ldots,9 \text{ if } \alpha_i>\text{Max}\left\{0,-\frac{R_1}{2F_1},-\frac{R_2}{2F_1}\right\} \quad \text{and}$$

$$\beta_i>\text{Max}\left\{0,\frac{\left(2F_1-R_3\right)}{2F_1},\frac{\left(2F_1-R_4\right)}{2F_1},\frac{-\alpha_i R_3}{\left(2\alpha_i F_1+R_1\right)},\frac{-\alpha_i R_4}{\left(2\alpha_i F_1+R_2\right)}\right\}.$$

Similarly, $P_2>0$ if $\gamma_2>\text{Max}\left\{0,\frac{d_6}{2F_1}\right\}$, $\delta_2>\text{Max}\left\{0,-\frac{d_5}{2F_3}\right\}$,

$$\alpha_j>\text{Max}\left\{0,-\frac{R_5}{2F_2},-\frac{R_6}{2F_2}\right\} \quad \text{and}$$

$$\beta_j>\text{Max}\left\{0,\frac{\left(2F_2-R_7\right)}{2F_2},\frac{\left(2F_2-R_8\right)}{2F_2},\frac{-\alpha_j R_7}{\left(2\alpha_j F_2+R_5\right)},\frac{-\alpha_j R_8}{\left(2\alpha_j F_2+R_6\right)}\right\}.$$

Similarly, $P_3 > 0$ if $\gamma_3 > \text{Max}\left\{0, \frac{d_2}{2F_2}\right\}, \delta_3 > \text{Max}\left\{0, -\frac{d_1}{2F_1}\right\}$,

$$\alpha_k > \text{Max}\left\{0, -\frac{R_9}{2F_3}, -\frac{R_{10}}{2F_3}\right\} \quad \text{and}$$

$$\beta_k > \text{Max}\left\{0, \frac{(2F_3 - R_{11})}{2F_3}, \frac{(2F_3 - R_{12})}{2F_3}, \frac{-\alpha_k R_{11}}{(2\alpha_k F_3 + R_9)}, \frac{-\alpha_k R_{12}}{(2\alpha_k F_3 + R_{10})}\right\}.$$

Theorem 2. *The C^1 triangular patch P, defined over the triangular domain D, in (3), is positive if the following sufficient conditions are satisfied:*

$$\alpha_i > \text{Max}\left\{0, -\frac{R_1}{2F_1}, -\frac{R_2}{2F_1}\right\}, \qquad \alpha_j > \text{Max}\left\{0, -\frac{R_5}{2F_2}, -\frac{R_6}{2F_2}\right\}, \qquad \alpha_k > \text{Max}\left\{0, -\frac{R_9}{2F_3}, -\frac{R_{10}}{2F_3}\right\},$$

$$\beta_i > \text{Max}\left\{0, \frac{(2F_1 - R_3)}{2F_1}, \frac{(2F_1 - R_4)}{2F_1}, \frac{-\alpha_i R_3}{(2\alpha_i F_1 + R_1)}, \frac{-\alpha_i R_4}{(2\alpha_i F_1 + R_2)}\right\},$$

$$\beta_j > \text{Max}\left\{0, \frac{(2F_2 - R_7)}{2F_2}, \frac{(2F_2 - R_8)}{2F_2}, \frac{-\alpha_j R_7}{\left(2\alpha_j F_2 + R_5\right)}, \frac{-\alpha_j R_8}{\left(2\alpha_j F_2 + R_6\right)}\right\},$$

$$\beta_k > \text{Max}\left\{0, \frac{(2F_3 - R_{11})}{2F_3}, \frac{(2F_3 - R_{12})}{2F_3}, \frac{-\alpha_k R_{11}}{(2\alpha_k F_3 + R_9)}, \frac{-\alpha_k R_{12}}{(2\alpha_k F_3 + R_{10})}\right\},$$

$$\gamma_1 > \text{Max}\left\{0, \frac{d_4}{2F_3}\right\}, \qquad \gamma_2 > \text{Max}\left\{0, \frac{d_6}{2F_1}\right\}, \qquad \gamma_3 > \text{Max}\left\{0, \frac{d_2}{2F_2}\right\},$$

$$\delta_1 > \text{Max}\left\{0, -\frac{d_3}{2F_2}\right\}, \qquad \delta_2 > \text{Max}\left\{0, -\frac{d_5}{2F_3}\right\}, \qquad \delta_3 > \text{Max}\left\{0, -\frac{d_1}{2F_1}\right\}.$$

The above constraints can be rearranged as

$$\alpha_i = l_1 + \text{Max}\left\{0, -\frac{R_1}{2F_1}, -\frac{R_2}{2F_1}\right\},$$

$$\alpha_j = l_2 + \text{Max}\left\{0, -\frac{R_5}{2F_2}, -\frac{R_6}{2F_2}\right\},$$

$$\alpha_k = l_3 + \text{Max}\left\{0, -\frac{R_9}{2F_3}, -\frac{R_{10}}{2F_3}\right\}, \qquad \beta_i = l_4 + \text{Max}\left\{0, \frac{(2F_1 - R_3)}{2F_1}, \frac{(2F_1 - R_4)}{2F_1}, \frac{-\alpha_i R_3}{(2\alpha_i F_1 + R_1)}, \frac{-\alpha_i R_4}{(2\alpha_i F_1 + R_2)}\right\},$$

$$\beta_j = l_5 + \text{Max}\left\{0, \frac{(2F_2 - R_7)}{2F_2}, \frac{(2F_2 - R_8)}{2F_2}, \frac{-\alpha_j R_7}{\left(2\alpha_j F_2 + R_5\right)}, \frac{-\alpha_j R_8}{\left(2\alpha_j F_2 + R_6\right)}\right\},$$

$$\beta_k = l_6 + \text{Max}\left\{0, \frac{(2F_3 - R_{11})}{2F_3}, \frac{(2F_3 - R_{12})}{2F_3}, \frac{-\alpha_k R_{11}}{(2\alpha_k F_3 + R_9)}, \frac{-\alpha_k R_{12}}{(2\alpha_k F_3 + R_{10})}\right\},$$

$$\delta_1 = l_7 + \text{Max}\left\{0, -\frac{d_3}{2F_2}\right\}, \qquad \delta_2 = l_8 + \text{Max}\left\{0, -\frac{d_5}{2F_3}\right\}, \qquad \delta_3 = l_9 + \text{Max}\left\{0, -\frac{d_1}{2F_1}\right\},$$

$$\gamma_1 = l_{10} + \text{Max}\left\{0, \frac{d_4}{2F_3}\right\}, \qquad \gamma_2 = l_{11} + \text{Max}\left\{0, \frac{d_6}{2F_1}\right\}, \qquad \gamma_3 = l_{12} + \text{Max}\left\{0, \frac{d_2}{2F_2}\right\},$$

where $l_i > 0, i = 1, 2, \ldots, 12$.

5. Demonstration

In this section, we shall illustrate the positivity preserving interpolating scheme developed in Section 4.

5.1. First example

We take the following function from [3]:

$$F_1(x, y) = \sin x \cos y + 0.91.$$

The positive data points are generated from the above function with the restriction of the domain as $[-3, 3] \times [-3, 3]$.

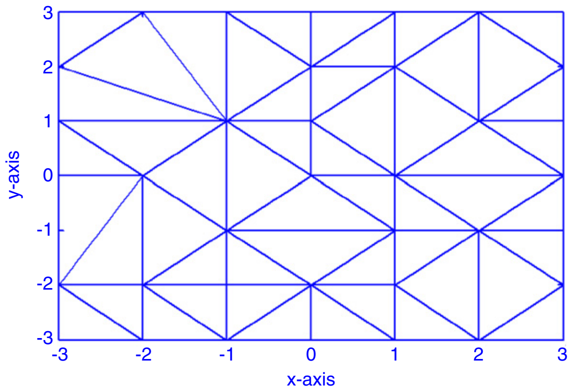

Fig. 2. Triangulation of the domain for $F_1(x, y)$.

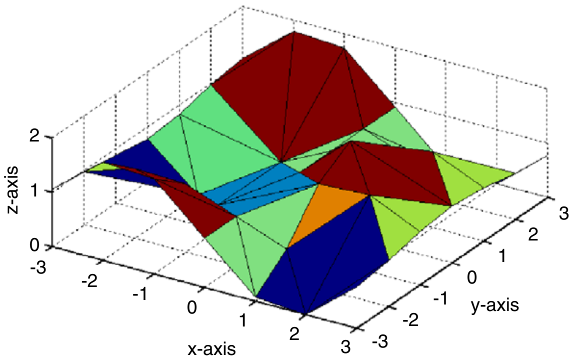

Fig. 3. Linear interpolation of the data generated from $F_1(x, y)$.

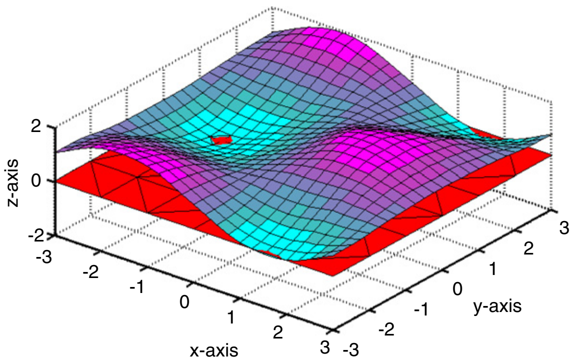

Fig. 4. Hermite triangular surface.

Fig. 2 is the Delaunay triangulation of the domain. Fig. 3 is the linear interpolation of the positive scattered data generated from the function $F_1(x, y)$. Fig. 4 is produced from (3) for the values of the free parameters $\gamma_i = \delta_i = 1, i = 1, 2, 3$, $\alpha_i = \alpha_j = \alpha_k = \beta_i = \beta_j = \beta_k = 1$. For these values of the free parameters the boundary and radial curves reduce to a standard cubic Hermite. From Fig. 4 it is clear that some part of the surface is lying below the plane $Z = 0$. Fig. 5 is another view of Fig. 4. Fig. 6 is generated from Theorem 2 with $l_i = 0.9, i = 1, \ldots, 12$. From Fig. 6 it is clear that the shape of the positive data is preserved in a pleasing way. Fig. 7 is obtained after the rotation of Fig. 6.

5.2. Second example

We take the following function from [5]:

$$F_2(x, y) = 5\left(1 + 2\exp\left(-3\left(\left(x^2 + y^2\right)^{\frac{1}{2}} - 6.7\right)\right)\right)^{-\frac{1}{2}}.$$

The positive data points are generated from the above function with the restriction of the domain as $[1, 9] \times [1, 9]$.

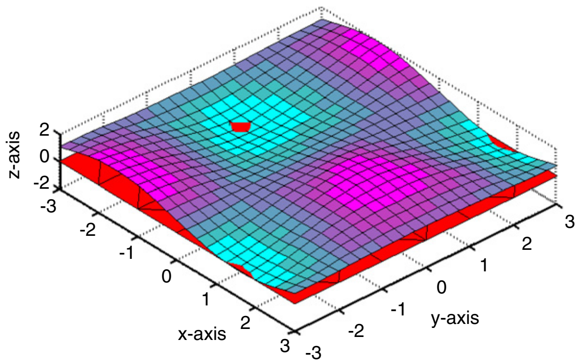

Fig. 5. Another view of Fig. 4.

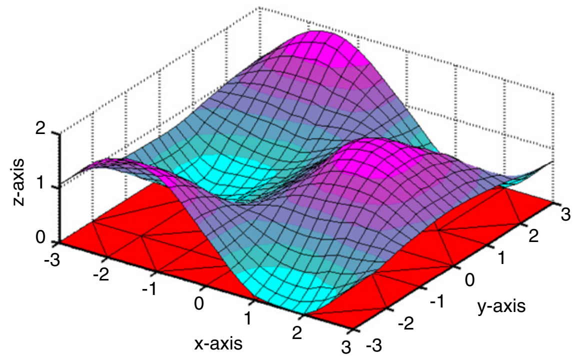

Fig. 6. The positive surface generated from Theorem 2 with $l_i = 0.9, i = 1, \ldots, 12$.

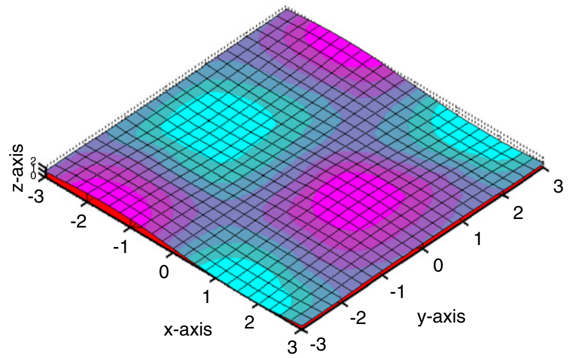

Fig. 7. Rotation of Fig. 6.

Figs. 8 and 9 are the Delaunay triangulation of the domain and linear interpolation of scattered data generated from the function $F_2(x, y)$, respectively. Fig. 10 is the Hermite triangular surface, produced from (3) for the values of the free parameters $\eta_i = \gamma_i = 1, i = 1, 2, 3, \alpha_i = \alpha_j = \alpha_k = \beta_i = \beta_j = \beta_k = 1$. From Fig. 10 it is clear that, for these values of the free parameters, (3) failed to preserve the positive shape of the data. Fig. 10 is rotated to Fig. 11 to make it more visible. Fig. 12 is generated from Theorem 2 with $l_i = 0.4, i = 1, \ldots, 12$. From Fig. 12 it is clear that the shape of the positive data is preserved using Theorem 2, and it is visually pleasing as well. Fig. 13 is another view of Fig. 12.

It is interesting to note that, in both the above examples, although the functions are provided, the derivatives are calculated from the derivative approximation scheme defined in [12] to test the ability of the positivity preserving scheme when derivatives are not provided.

6. Conclusion

A C^1 local side-vertex scheme is developed to preserve the shape of positive scattered data. The C^1 rational cubic function is used as both the side-vertex interpolant and the boundary curve interpolant. This rational cubic function involves two free

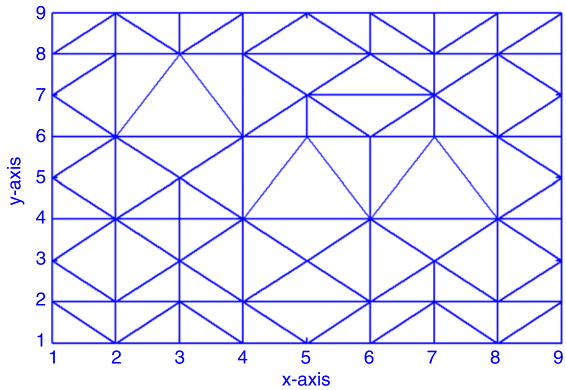

Fig. 8. Triangulation of the domain for $F_2\,(x, y)$.

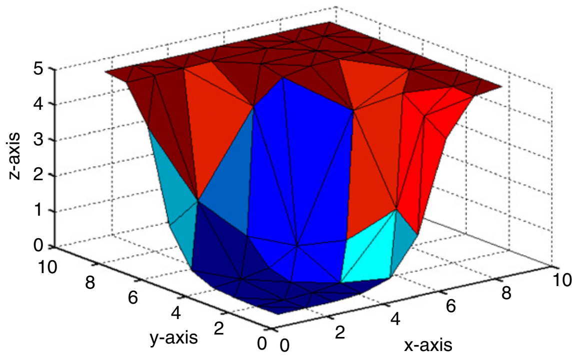

Fig. 9. Linear interpolation of the data generated from $F_2\,(x, y)$.

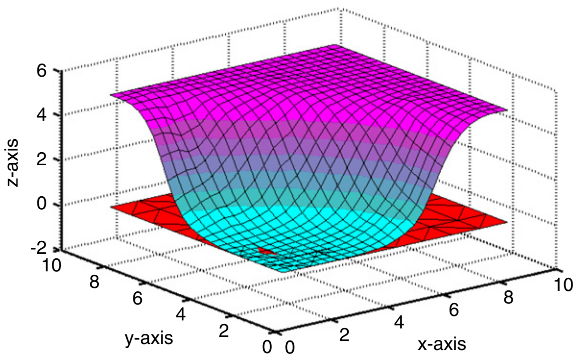

Fig. 10. Hermite triangular surface.

parameters in its construction, yielding 12 free parameters in each triangular patch. Data dependent sufficient conditions are derived on these free parameters to preserve the shape of the positive scattered data. The domain is triangulated by the Delaunay triangulation method. The partial derivatives at the vertices of triangles are estimated by the local derivative estimation scheme. But, in general, the choice of the derivative is left to the decision of the user as well. Thus the method is equally applicable to data with and without derivatives. The proposed scheme is demonstrated over different data sets.

The scheme of this paper has many advantageous features over existing schemes. The schemes developed in [2–4,6] were not applicable to data with derivatives, whereas the scheme developed in this paper is applicable to data both with and without derivatives. In this paper the derivatives are estimated by the derivative estimation scheme proposed in [12]. In [5], a 1-parameter rational cubic function was used as a side-vertex, boundary interpolant and the value of the parameter that reduced the rational cubic function to a cubic Hermite was used in all the triangular patches. If the Hermite triangular patches lost positivity, a global maximum value was assigned to all these parameters of each triangle interpolant to ensure that the resulting surface was non-negative. The method developed in [5] is not local whereas our scheme is local.

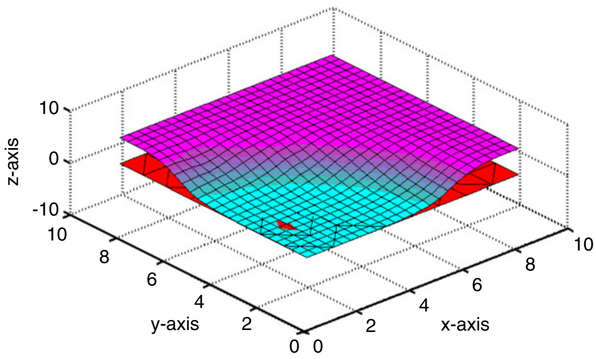

Fig. 11. Another view of Fig. 10.

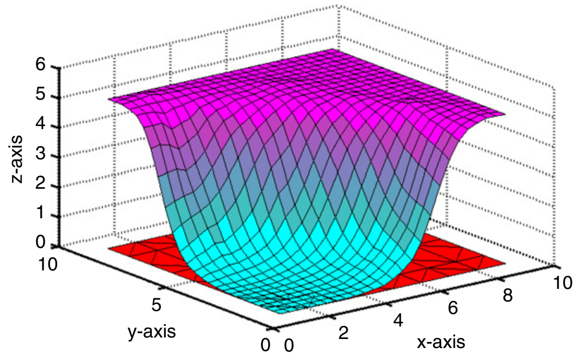

Fig. 12. The positive surface generated from Theorem 2 with $l_i = 0.4$, $i = 1, \dots, 12$.

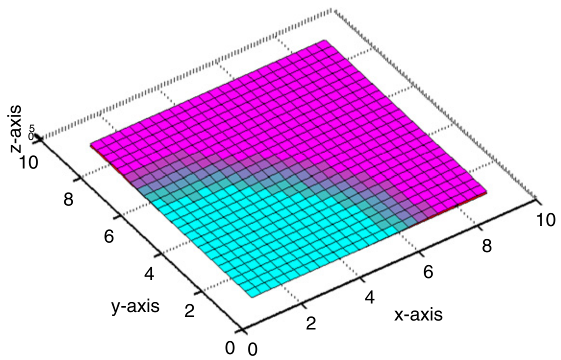

Fig. 13. Another view of Fig. 12.

Surface construction schemes involving shape parameters are suitable to data having singularities, whereas ordinary polynomials are not.

The development of monotonicity and convexity preservation schemes for the scattered data is an interesting task. The authors are in the process of completing this in a subsequent paper.

References

[1] M.R. Asim, G. Mustafa, K. Brodlie, Constrained visualization of 2D positive data using modified quadratic Shepard method, in: WSCG Posters Proceedings, 2–6 February 2004, Plzen, Czech Republic, Union Agency — Science Press, 2004.

[2] E.S. Chan, B.H. Ong, Range restricted scattered data interpolation using convex combination of cubic Bézier triangles, Journal of Computational and Applied Mathematics 136 (2001) 135–147.

[3] V.P. Kong, B.H. Ong, K.H. Saw, Range restricted interpolation using cubic Bézier triangles, in: WSCG, 2–6 Feb. 2004, Plzen Czech Republic, Union Agency — Science Press, 2004.

[4] B. Mulansky, J.W. Schmidt, Nonnegative C^1 interpolation of scattered data using Powell–Sabin splines, Preprint MATH-NM-02-1993, Technical University Dresden, 1993.

[5] B.H. Ong, H.C. Wong, A C^1 positivity preserving scattered data interpolation scheme, in: F. Fontanella, K. Jetter, P.J. Laurent (Eds.), Advanced Topics in Multivariate Approximation, 1996, pp. 259–274.

[6] A.R.M. Piah, T.N.T. Goodman, K. Unsworth, Positivity-preserving scattered data interpolation, Lecture Notes in Computer Science 3604 (2005) 336–349.
[7] G. Nielson, The side–vertex method for interpolation in triangles, Journal of Approximation Theory 25 (1979) 318–336.
[8] M. Tian, Y. Zhang, J. Zhu, Q. Duan, Convexity-preserving piecewise rational cubic interpolation, in: ISCIAS, Hefei, China, 2005.
[9] M.Z. Hussain, M. Sarfraz, Positivity-preserving interpolation of positive data by rational cubics, Journal of Computational and Applied Mathematics 218 (2) (2008) 446–458.
[10] M.Z. Hussain, J.M. Ali, Positivity preserving piecewise rational cubic interpolation, Matematika 22 (2) (2006) 147–153.
[11] T.P. Fang, L.A. Piegl, Algorithms for Delaunay triangulation and convex-hull computation using a sparse matrix, Computer Aided Design 24 (1992) 425–436.
[12] T.N.T. Goodman, H.B. Said, L.H.T. Chang, Local derivative estimation for scattered data interpolation, Applied Mathematics and Computation 68 (1995) 41–50.
[13] K.W. Brodlie, S. Butt, Preserving positivity using piecewise cubic interpolation, Computers and Graphics 17 (1) (1993) 55–64.
[14] R. Franke, G. Nielson, Smooth interpolation of large set of scattered data, International Journal of Numerical Methods in Engineering 15 (1980) 1691–1704.
[15] A. Saaban, A.R.M. Piah, A.A. Majid, L.H.T. Chang, G^1 scattered data interpolation with minimized sum of squares of principal curvatures, International Journal of Computer Graphics and CAD/CAM 1 (1–4) (2005) 82–92.
[16] M. Sarfraz, M. Al-Mulhem, F. Ashraf, Preserving monotonic shape of the data using piecewise rational cubic functions, Computers and Graphics 21 (1) (1997) 5–14.